Validation of EarthCARE aerosol products from ATLID and MSI with remote sensing measurements at the Lampedusa Station for Climate Observations, Italy

D. Meloni[1,*], T. Di Iorio[1], G. Pace[1], F. Anello[2], L. De Silvestri[1], A. di Sarra[3], F. Monteleone[2], S. Piacentino[2], D. Sferlazzo[4]

Department of Sustainability, ENEA, Italy, [1]Rome, 00123; [2]Palermo, 90139; [3]Frascati, 00044; [4]Lampedusa, 92031

*daniela.meloni@enea.it

Figure 1. *The ENEA Station for Climate Observations at Lampedusa Island.*

Introduction

The ENEA Station for Climate Observations at Lampedusa Island (35.52° N, 12.63° E, ***www.lampedusa.enea.it***) participate in the validation activities of the EarthCARE (EC) mission Commissioning phase in the framework of the EC-Valmed.it project, funded by the Italian Space Agency. The measurements from Raman-Mie-Rayleigh lidar and a solar/lunar/sky AERONET photometer, contributing to ACTRIS Research Infrastructure, are used in this work.

Preliminary studies have shown that the remote sensing measurements at Lampedusa are representative of a wide marine region, making it an ideal site for validation of satellite observations.

For additional information on the results of the EC-Valmed.it project see the posters P010 by E. Adirosi et al., P028 by D. Meloni et al., P035 by S. Sensi et al., and P057 by G. Pace et al.

Methodology and data selection

Validation of L2a and L2b aerosol products against AERONET level 1.5 aerosol optical depth (AOD) and lidar extinction, backscattering and depolarization profiles from July 2024 to May 2026. EC and ground-based data selection are shown in **Figure 2** and **Table 1**.

L2a: ATLID AOD at 355 nm from **A-ALD**;

ATLID aerosol extinction, backscattering and depolarization profiles at 355 nm from **A-EBD**;

MSI AOD at 670 nm (for land and ocean), AOD at 865 nm (only for ocean), and the corresponding Ångström exponent (AE) from **M-AOT**.

L2b: ATLID and MSI AOD at 355, 670, and 865 nm, AE(355,670) and AE(670,865) from **AM-ACD** product.

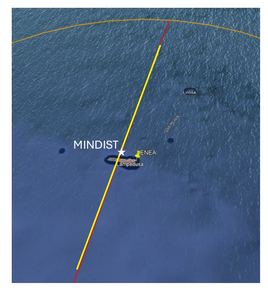

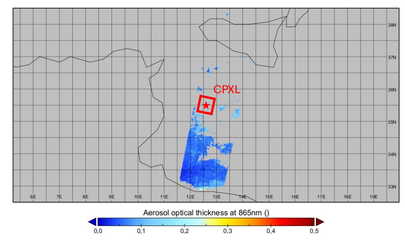

Figure 2. *Representation of ATLID data selection around MINDIST point and MSI data around the CPXL pixel. One daytime and one nighttime ATLID overpasses have MINDIST<10 km*

Table 1. *Criteria for EC and ground-based data selection. MINDIST: minimum ATLID ground track - Lampedusa observatory distance; CPXL: MSI pixel closest to Lampedusa observatory*

A-EBD	LIDAR	A-ALD	AERONET	M-AOT	AERONET	AM-ACD	AERONET
Ext, bsc, depol. 355 nm	**Ext, bsc, depol. 355 nm or 532 nm**	**AOD355**	**AOD340**	**AOD670, AOD865, AE**	**AOD675, AOD870, AE**	**AOD355, AOD670, AOD865, AE(355,670), AE(670,865)**	**AOD340, AOD675, AOD870, AE(340,675), AE(675,870)**
Time(MINDIST) ±1 pixel	Time(MINDIST) ±2.5 min.	Time(MINDIST) ±10 s	Time(MINDIST) ±60 min.	51x51or 101x101 pixel area centred at (CPXL)	Time(CPXL) ±60 min.	51x51 pixel area centred at (CPXL)	Time(CPXL) ±60 min.
QS 0 (good quality)		QS 0 (good quality)		QS 0 (good/nominal quality)		QS 0 (good data) and 1 (valid data, but aerosol not confined in a dominant layer)	

Results

ATLID extinction and depolarization profiles

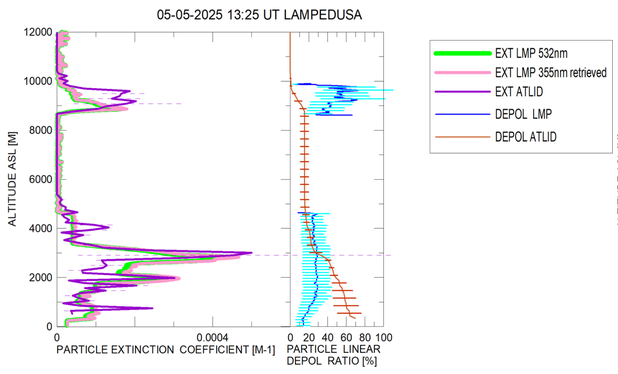

Figure 3. *Vertical Profiles of aerosol extinction coefficient and particle linear depolarization ratio retrieved by ATLID and Lampedusa LIDAR during the 5 May 2025 overpass.*

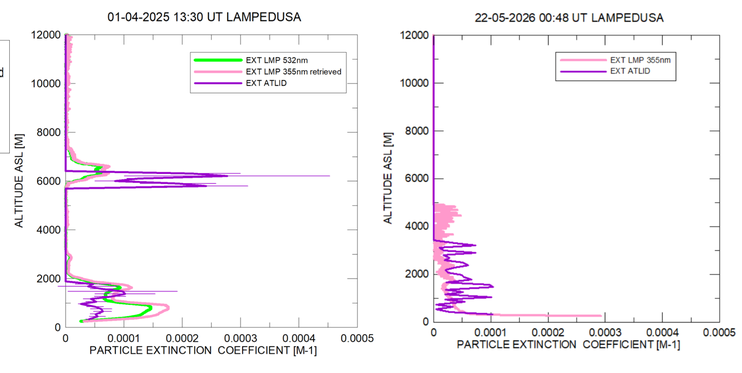

Figure 4. *Vertical Profiles of aerosol extinction coefficient retrieved by ATLID and Lampedusa LIDAR during the 1 April 2025 daytime overpass (LEFT PANEL) and during the22 May 2026 nighttime overpass(RIGHT PANEL)*

Three different overpasses are represented in the figures on the left. **Figure 3** shows the extinction profiles for 5 May 2025 overpass (AOD355=0.604, MINDIST=1.8 km), characterized by an intense Saharan dust transport, while **Figure 4** shows on LEFT panel the 1 April 2025 overpass (AOD355=0.203, MINDIST=80.4 km). And on RIGHT panel the 355 nm extinction coefficient profiles of 22 May 2026 nighttime overpass (MINDIST=5.4 km) . The corresponding ATLID vertical profiles are averages of 3 profiles centered at the time of MINDIST. A high thin cloud is present above the aerosol layer, detected by both instruments, during 2 overpasses

For the 2025 overpasses, the vertical profile of the extinction coefficient at 355 nm is derived from the measurements of the Lampedusa LIDAR at 532 nm using the spectral AERONET AODs and AE data at the time of MINDIST (13:25-13:30 UT). During 2026 overpass the 355 nm elastic signal is measured by the Lampedusa LIDAR and the extinction coefficient at 355 nm is carried out.

The particle depolarization ratio profiles are also shown for LAMPEDUSA LIDAR and ATLID for 5 May 2025. The large values of the particle depolarization ratio are representative for desert dust aerosols, but agree only in the 2.8-4.8 km layer.

L2a and L2b ATLID and MSI AOD355, AOD670, AOD865, and AEs

AODs

The AM-ACD AOD355 is more scattered compared to the A-ALD AOD(355), with some points underestimating the AERONET AOD(340). However, unlike the A-ALD product which has to be filtered for too high values of AOD355 and errAOD355, no filter has been applied to the AM-ACD product.

When comparing AOD with MSI, the 51x51 pixel area for AM-ACD has been considered since it is comparable with the 101x101 pixel area for M-AOT.

For AM-ACD most of the available data correspond to areas including Lampedusa. This implies fewer matchups than for M-AOT and a better agreement.

The matchups corresponding to AOD675 and AOD870 from AERONET above 0.32 and 0.28 (left plots in **Figure 5**), respectively, are no longer present in the AM-ACD scatterplot.

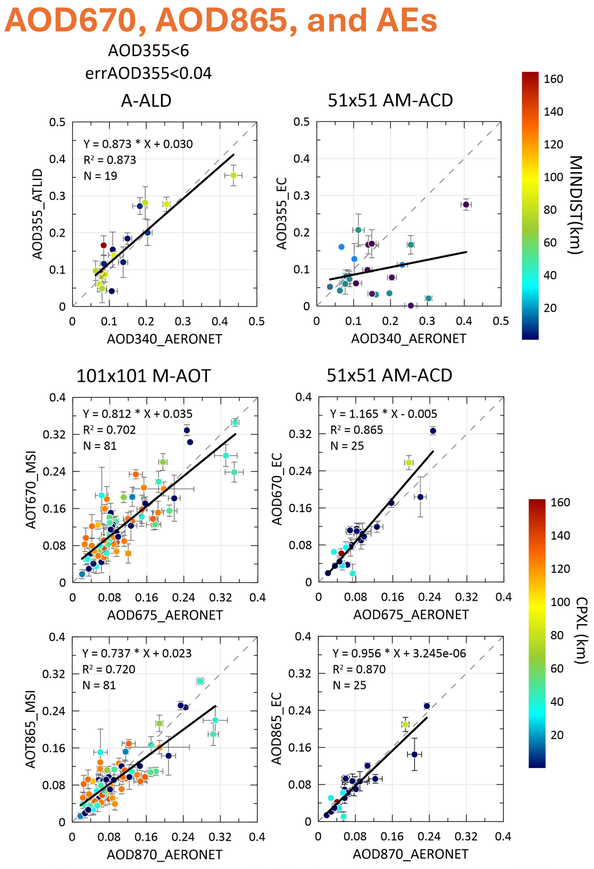

Figure 5. *Scatterplot of AODs from L2a (left plots) and L2b (right plots). Bars represent one standard deviation.*

AEs

The AE(670,865) from M-AOT and from AM-ACD have been compared with the AERONET AE(675,870) (**Figure 6**) selecting only those case for which AOD670_EC>0.1.

Both EC products show an AE overestimation.

The AE(355,670) from AM-ACD has been compared with the AERONET AE(340,675) (**Figure 7**) selecting only those case for which AOD670_EC>0.1.

Only few matchups are available, some of which show negative EC values, in two cases associated to AOD355<0.1.

In two cases (not shown) the AE(355,670) values are severely low: on 30 July 2024, with average AOD355=0.001 and AE(355,670)=-6.9, and on 6 May 2026, with average AOD355=0.02 and AE(355,670)=-4.3.

In these cases, no agreement is found between the MSI and ATLID dominant aerosol type and all the AE values in the frame are negative.

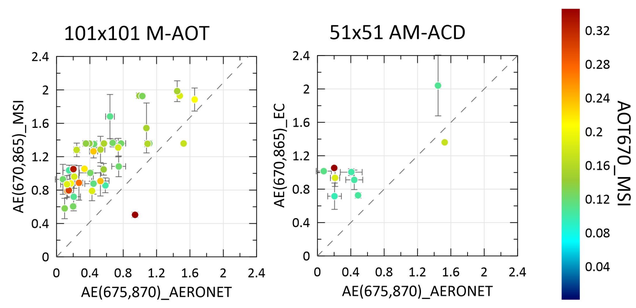

Figure 6. *Scatterplot of AE(670,865) from L2a (left) and L2b (right). Bars represent one standard deviation.*

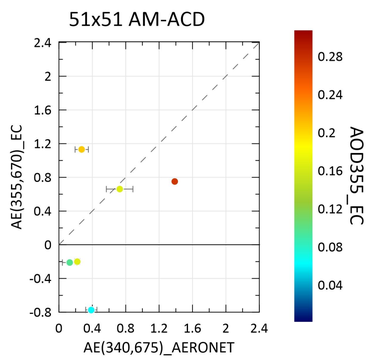

Figure 7. *Scatterplot of AE(355,670) from L2b. Bars represent one standard deviation.*

Acknowledgements

This work was supported by the ASI EC-ValMed.It project (Agreement n. 2024-1-HB.0). It is part of the activity carried out in the frame of the ESA projects EVID05 and EVID11.

The support of ACTRIS-ERIC and University of Valladolid concerning the AERONET photometer calibration is gratefully acknowledged, as well as NASA for data processing.

The authors would like to acknowledge COST Actions HARMONIA (CA21119) and EARLICOST (CA24135), supported by COST (European Cooperation in Science and Technology).

EarthCARE 2026 Science and Validation workshop

8–12 June 2026 | Rhodes House | Oxford, UK